

Partial order in frustrated quantum spin systems

R. Quartu and H. T. Diep

Groupe de Physique Statistique, Université de Cergy-Pontoise, 2, Avenue Adolphe Chauvin, 95302 Cergy-Pontoise Cedex, France

(Received 7 May 1996; revised manuscript received 9 September 1996)

We show in this paper the frustration effect on the magnetic properties of a body-centered-cubic lattice with mixed quantum Heisenberg spins. The classical ground-state (g.s.) is determined as a function of spin amplitudes and nearest-neighbor and next-nearest neighbor interactions. Various noncollinear g.s.'s are found. The quantum behavior of collinear and noncollinear phases at zero and finite temperatures is then studied using the Green function formalism which allows us to calculate self-consistently different properties. A general phase diagram is shown. One of the striking results is the existence of a partially ordered phase at finite temperature due to the frustration. [S0163-1829(97)11005-0]

I. INTRODUCTION

The frustration effect has received increasing attention during the last decade. Frustrated spin systems often have noncollinear ground-state (g.s.) spin configurations which cause difficulties in the calculation of their properties. Many established theoretical methods fail to give a correct behavior of such systems. It is known that competing interactions give rise to frustration which, in turn, causes many spectacular phenomena in spin systems such as a high ground-state degeneracy, noncollinear spin configurations, reentrance, partial disorder, the controversial nature of the phase transition, etc. For a recent review on different aspects of the frustration effect, the reader is referred to Ref. 1.

The purpose of this paper is to study the properties of a body-centered-cubic (bcc) lattice with a quantum Heisenberg spin of general amplitudes. We take into account the nearest-neighbor (NN) and next-nearest-neighbor (NNN) interactions.

In Sec. II we present the model and the mathematical method: We first show the g.s. configuration and then work out a general Green function's formalism to study their magnetic properties at finite temperatures. Applications are given in Sec. III where a phase diagram is shown. We find here that partial disordering exists at equilibrium in our quantum mixed spin system. Discussion on the frustration effect is given.

II. MODEL AND MATHEMATICAL FORMULATION

We consider a two-sublattice body-centered cubic (bcc). We divide the magnetic bcc lattice into two sc sublattices A and B . To be general, let us suppose that each lattice point of the A sublattice is occupied by a spin of magnitude S_A and each lattice point of the B sublattice by a spin of magnitude S_B . S_A and S_B are arbitrary. In studying such a general case, we can apply our results to the case of ferrimagnet where S_A is different from S_B . This case is interesting because, unlike the ferromagnets and antiferromagnets, there has been only a very limited number of works on ferrimagnets. This is due perhaps to the fact that ferrimagnetic crystals usually have complicated lattice structures.² In particular, there have been some calculations of spin waves.²⁻⁶ All

of these have been restricted to the zero-temperature case and a collinear spin configuration.

We consider the model system described by the following Hamiltonian:

$$H = 2J_1 \sum_{\langle ij \rangle} \mathbf{S}_i \cdot \mathbf{S}_j + 2J_{2A} \sum_{\langle ij \rangle_2} \mathbf{S}_i \cdot \mathbf{S}_j + 2J_{2B} \sum_{\langle ij \rangle_2} \mathbf{S}_i \cdot \mathbf{S}_j + 2 \sum_i d_i S_i^z, \quad (1)$$

where $\sum_{\langle ij \rangle}$ indicates the sum over the NN spin pairs and $\sum_{\langle ij \rangle_2}$ that over the NNN pairs, J_1 denotes the NN exchange coupling, and $J_{2A(B)}$ the NNN exchange coupling between spins of the sublattice $A(B)$. The last term is a very small stabilizing field pointed along the local z axis of the i th spin that we introduce for numerical calculational convenience. Let us use the notation $\epsilon_{A(B)} = J_{2A(B)}/J_1$. The classical g.s. can be determined by minimizing the interaction energy, taking into account the hard spin conditions; i.e., S_A and S_B are constant (variational method). The result is that the unit cell is composed of two cubes as shown in Fig. 1 with four spins denoted as $A, A', B,$ and B' . Let us describe the g.s. configuration.

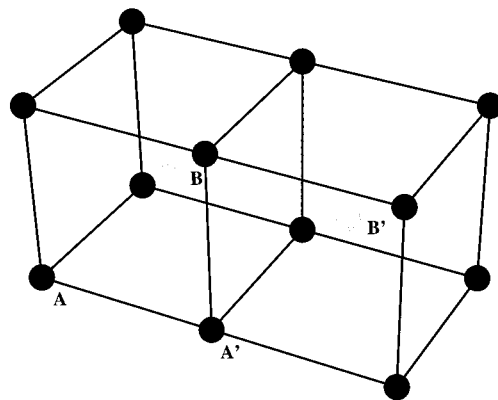


FIG. 1. Magnetic unit cell composed of two cubes. A (B) spins are shown by black (gray) circles.

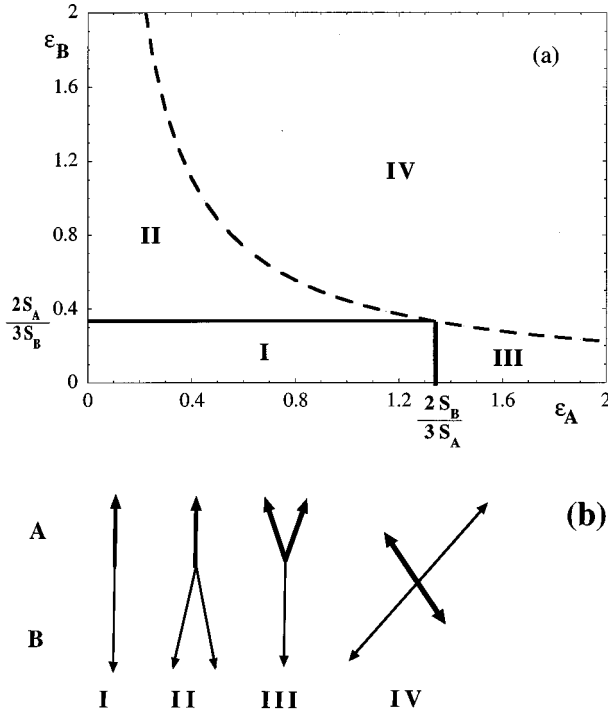


FIG. 2. (a) g.s. phase diagram plotted by taking $S_A=0.5$ and $S_B=1$. See text for description. (b) Four g.s. spin configurations corresponding, respectively, to zones I–IV of (a). A (B) spins are shown by short (long) and thick (thin) arrows. See text for detail.

(1) Independent antiferromagnetic subsystems [zone IV of Fig. 2(a)]: The A-spin subsystem is independent of the B-spin one if $\epsilon_A \epsilon_B > \frac{4}{9}$ (dashed curve in the figure shows $\epsilon_A \epsilon_B = \frac{4}{9}$). In this case we have $\mathbf{S}_B = -\mathbf{S}_{B'}$, and $\mathbf{S}_A = -\mathbf{S}_{A'}$, where Θ_{AB} , being the angle between \mathbf{S}_A and \mathbf{S}_B , is arbitrary. This is schematically shown by the right configuration Fig. 2(b).

(2) Collinear configuration [zone I of Fig. 2(a)]: This is the case when $\epsilon_A < \frac{2}{3} S_B / S_A$ and $\epsilon_B < \frac{2}{3} S_A / S_B$. The resulting spin configuration is $\mathbf{S}_A = \mathbf{S}_{A'}$, $\mathbf{S}_B = \mathbf{S}_{B'}$, and \mathbf{S}_A is antiparallel to $\mathbf{S}_{B'}$. The collinear configuration is shown on the left in Fig. 2(b).

(3) Noncollinear configuration of B spins [zone II of Fig. 2(a)]: If $\epsilon_B > \frac{2}{3} S_A / S_B$ and $\epsilon_A < \frac{2}{3} S_B / S_A$, then $\mathbf{S}_A = \mathbf{S}_{A'}$, and $\mathbf{S}_B \neq \mathbf{S}_{B'}$, with

$$\cos(\Theta_{AB}) = -\frac{2}{3} \frac{S_A}{\epsilon_B S_B}$$

and

$$\cos(\Theta_{BB'}) = 2 \left(\frac{2}{3} \frac{S_A}{\epsilon_B S_B} \right)^2 - 1,$$

where $\Theta_{BB'}$ is the angle between \mathbf{S}_B and $\mathbf{S}_{B'}$. This is shown by the second from left in Fig. 2(b).

(4) Noncollinear configuration of A-spins [zone III of Fig. 2(a)]: if $\epsilon_A > \frac{2}{3} S_B / S_A$ and $\epsilon_B < \frac{2}{3} S_A / S_B$, then $\mathbf{S}_B = \mathbf{S}_{B'}$, $\mathbf{S}_A \neq \mathbf{S}_{A'}$, with

$$\cos(\Theta_{AB}) = -\frac{2}{3} \frac{S_B}{\epsilon_A S_A}$$

and

$$\cos(\Theta_{AA'}) = 2 \left(\frac{2}{3} \frac{S_B}{\epsilon_A S_A} \right)^2 - 1,$$

where $\Theta_{AA'}$ is the angle between \mathbf{S}_A and $\mathbf{S}_{A'}$. This is shown by the third from left in Fig. 2(b). Now we choose, for each spin, the local z axis along its spin quantification axis.⁷ We note that the local z -axis direction can change with the temperature upon iteration as seen below. We can rewrite the Hamiltonian in the local framework as

$$\begin{aligned} H = 2 \sum_{\langle kl \rangle} & \frac{1}{4} J_{kl} [\cos(\Theta_{kl}) - 1] (S_k^+ S_l^+ + S_k^- S_l^-) \\ & + \frac{1}{4} J_{kl} [\cos(\Theta_{kl}) + 1] (S_k^+ S_l^- + S_k^- S_l^+) \\ & + J_{kl} \cos(\Theta_{kl}) S_k^z S_l^z + \frac{1}{2} J_{kl} \sin(\Theta_{kl}) (S_k^+ + S_k^-) S_l^z \\ & + \frac{1}{2} J_{kl} \sin(\Theta_{lk}) (S_l^+ + S_l^-) S_k^z + 2 \sum_i d_i S_i^z, \end{aligned} \quad (2)$$

where Θ_{kl} is the angle between the two spins at the lattice sites k and l . Equation (2) is valid for collinear and noncollinear configurations. Following Tahir-Kheli and de ter Haar,⁸ we define two double-time Green's functions by

$$\begin{aligned} G_{ij}^{\pm}(t, t') &= \langle \langle S_i^{\pm}(t); S_j^{\mp}(t')^n S_j^{\pm}(t')^{n-1} \rangle \rangle, \\ F_{ij}^{\pm}(t, t') &= \langle \langle S_i^{\pm}(t); S_j^{\pm}(t')^n S_j^{\mp}(t')^{n-1} \rangle \rangle, \end{aligned} \quad (3)$$

where $n = 1, \dots, 2S_{A(B)}$. The equations, of motion for $G_{ij}(t, t')$ and $F_{ij}(t, t')$ read

$$\begin{aligned} i \frac{d}{dt} G_{ij}^{\pm}(t, t') &= \langle [S_i^{\pm}(t), S_j^{\mp}(t')^n S_j^{\pm}(t')^{n-1}] \rangle \\ & - \langle \langle [H, S_i^{\pm}(t)]; S_j^{\mp}(t')^n S_j^{\pm}(t')^{n-1} \rangle \rangle, \\ i \frac{d}{dt} F_{ij}^{\pm}(t, t') &= \langle [S_i^{\pm}(t), S_j^{\pm}(t')^n S_j^{\mp}(t')^{n-1}] \rangle \\ & - \langle \langle [H, S_i^{\pm}(t)]; S_j^{\pm}(t')^n S_j^{\mp}(t')^{n-1} \rangle \rangle, \end{aligned} \quad (4)$$

and we have

$$[S_i^+, S_j^{-n} S_j^{+n-1}] = u_i(n) \delta_{ij}, \quad (5)$$

$$[S_i^-, S_j^{-n} S_j^{+n-1}] = 0, \quad (6)$$

where $u_i(n)$ is a function of S_i^z .⁸ As Tyablikov, we neglect the higher orders of correlation. Then, we have

$$\begin{aligned} & \langle \langle S_k^z S_i^{\pm}(t); S_j^{\mp}(t')^n S_j^{\pm}(t')^{n-1} \rangle \rangle \\ & = \langle S_k^z \rangle \langle \langle S_i^{\pm}(t); S_j^{\mp}(t')^n S_j^{\pm}(t')^{n-1} \rangle \rangle, \\ & \langle \langle S_k^+ S_i^{\pm}(t); S_j^{\mp}(t')^n S_j^{\pm}(t')^{n-1} \rangle \rangle \\ & = \langle S_k^+ \rangle \langle \langle S_i^{\pm}(t); S_j^{\mp}(t')^n S_j^{\pm}(t')^{n-1} \rangle \rangle = 0 \end{aligned} \quad (7)$$

Furthermore, since we work at the first order, we have

$$\langle \langle S_i^z; S_j^{\mp}(t')^n S_j^{\pm}(t')^{n-1} \rangle \rangle = 0. \quad (8)$$

We now introduce the Fourier transforms

$$G_{ij}^{\pm}(t, t') = \frac{1}{\pi^3} \int \int \int_0^{\pi} d\mathbf{k} \frac{1}{2\pi} \times \int_{-\infty}^{+\infty} d\omega e^{-i\omega(t-t')} g^{\pm}(\omega, \mathbf{k}) e^{i\mathbf{k} \cdot (\mathbf{i}-\mathbf{j})}. \quad (9)$$

The Fourier transforms of the retarded Green's functions satisfy a set of equations readily to be rewritten under a matrix form. There are four atoms in a magnetic cell as seen by the g.s. configuration shown above (Fig. 1). Therefore, eight Green functions have to be defined. The explicit forms of these functions are too lengthy to write down here. We give only one of them:

$$\begin{aligned} \omega g^{\pm AA'} &= u^{\pm} - \{ \mp J_1 [\cos(\Theta_{AB}) + 1] \lambda_A \mu_A g^{\pm BA} \mp J_1 [\cos(\Theta_{AB'}) + 1] \lambda_{A'} \mu_{A'} g^{\pm B'A} \mp J_1 [\cos(\Theta_{AB}) - 1] \lambda_A \mu_A g^{\mp BA} \\ &\quad \mp J_1 [\cos(\Theta_{AB'}) - 1] \lambda_{A'} \mu_{A'} g^{\mp B'A} \mp J_2^A [\cos(\Theta_{AA'}) - 1] 4 \gamma_2 \mu_A g^{\mp A'A} \\ &\quad \mp J_2^A [\cos(\Theta_{AA'}) + 1] 4 \gamma_2 \mu_A g^{\pm A'A} \pm 2B^A g^{\pm AA'} \}. \end{aligned}$$

The constants are defined by

$$u^+ = u,$$

$$u^- = 0,$$

$$\mu_{A(B)} = \langle S_{A(B)}^z \rangle,$$

$$\lambda_A = e^{i(k_x a + k_y a)/4} + e^{-i(k_x a + k_y a)/4} + e^{-i k_z a/2} (e^{i(k_x a - k_y a)/4} + e^{-i(k_x a - k_y a)/4}),$$

$$\lambda'_A = e^{i(k_x a - k_y a)/4} + e^{-i(k_x a - k_y a)/4} + e^{-i k_z a/2} (e^{i(k_x a + k_y a)/4} + e^{-i(k_x a + k_y a)/4}),$$

$$\lambda_B = e^{+i k_z a/2} (e^{i(k_x a + k_y a)/4} + e^{-i(k_x a + k_y a)/4}) + e^{i(k_x a - k_y a)/4} + e^{-i(k_x a - k_y a)/4},$$

$$\lambda'_B = e^{+i k_z a/2} (e^{i(k_x a - k_y a)/4} + e^{-i(k_x a - k_y a)/4}) + e^{i(k_x a + k_y a)/4} + e^{-i(k_x a + k_y a)/4},$$

$$\gamma_2 = \frac{\cos(\frac{1}{2} k_x a) + \cos(\frac{1}{2} k_y a) + \cos(\frac{1}{2} k_z a)}{2}$$

$$\begin{aligned} B^A &= 4J_1 [\mu_B \cos(\Theta_{AB}) + \mu_{B'} \cos(\Theta_{AB'})] \\ &\quad + 6J_2^A \mu_{A'} \cos(\Theta_{AA'}) + d_A, \end{aligned} \quad (10)$$

a being the lattice constant of the bcc crystal, i.e., the distance between NN spins of the same sublattice.

By symmetry, we note that $\cos(\Theta_{BB'}) = \cos(2\pi - 2\Theta_{AB}) = \cos(2\Theta_{AB})$ and $g_{A'} = g_A$, $\langle S_{A'}^z \rangle = \langle S_A^z \rangle$, $g_{B'} = g_B$, $\langle S_{B'}^z \rangle = \langle S_B^z \rangle$.

The set of equations obtained by writing the equations of the type Eq. (10) for all the Green functions can be applied to any phase shown in Fig. 2(b) with an appropriate choice of Θ_{ij} . Solving these equations, we obtain the spin-wave spectrum of the present system:

$$\omega_{\pm}^{\pm} = \sqrt{W1 \pm \sqrt{W2}},$$

$$\omega_{\pm}^{\pm} = -\sqrt{W1 \pm \sqrt{W2}},$$

$$W1 = A_A^2 + A_B^2 + 2Z_{AB} \cos(\Theta_{AB}) - [C_B \sin(\Theta_{AB})]^2,$$

$$\begin{aligned} W2 &= \{A_A^2 - A_B^2 + [C_B \sin(\Theta_{AB})]^2\}^2 + 4Z_{AB} \{A_A + \cos(\Theta_{AB}) \\ &\quad \times [A_B - C_B \sin(\Theta_{AB})]^2\} \{A_A \cos(\Theta_{AB}) \\ &\quad + [A_B + C_B \sin(\Theta_{AB})]^2\}, \end{aligned} \quad (11)$$

where

$$A_A = 16J_1 \mu_B \cos(\Theta_{AB}) + (12J_2^A - 8J_2^A \gamma_2) \mu_A + 2d_B,$$

$$\begin{aligned} A_B &= 16J_1 \mu_A \cos(\Theta_{AB}) + [12J_2^B \cos(2\Theta_{AB}) \\ &\quad - 8J_2^B \gamma_2 \cos(\Theta_{AB})^2] \mu_B + 2d_A, \end{aligned}$$

$$C_B = 8J_2^B \mu_B \gamma_2,$$

$$Z_{AB} = (16\gamma_1)^2 \mu_A \mu_B,$$

$$\gamma_1 = \cos(k_x a/4) \cos(k_y a/4) \cos(k_z a/4). \quad (12)$$

Using the spectral theorem which relates the correlation function $\langle S_i^{-n} S_j^{+n} \rangle$ to the Green's functions,⁹ one has

$$\begin{aligned} \langle S_i^{-n} S_j^{+n} \rangle &= \lim_{\eta \rightarrow 0} \frac{1}{\pi^3} \int_0^{\pi} \int_0^{\pi} \int_0^{\pi} d\mathbf{k} \int_{-\infty}^{+\infty} \frac{i}{2\pi} [g^+(\omega + i\eta) \\ &\quad - g^+(\omega - i\eta)] \frac{d\omega}{e^{\beta\omega} - 1} e^{i\mathbf{k} \cdot (\mathbf{i}-\mathbf{j})}, \end{aligned} \quad (13)$$

where η is an infinitesimal positive constant and $\beta = 1/k_B T$, k_B being the Boltzmann constant. The solution for all Green functions is lengthy to write down here. We give only one of them:

$$\begin{aligned}
g_{AA}^+ &= \frac{2u_A}{|\Delta(\omega)|} \left[A_A A_B^2 - A_B^2 \omega - A_A \omega^2 + \omega^3 \right. \\
&\quad - A_B Z_{AB} \cos\left(\frac{\Theta_{AB}}{2}\right)^4 \\
&\quad - \omega Z_{AB} \cos\left(\frac{\Theta_{AB}}{2}\right)^4 - A_B Z_{AB} \sin\left(\frac{\Theta_{AB}}{2}\right)^4 \\
&\quad + \omega Z_{AB} \sin\left(\frac{\Theta_{AB}}{2}\right)^4 - 8C_B Z_{AB} \cos\left(\frac{\Theta_{AB}}{2}\right)^4 \sin\left(\frac{\Theta_{AB}}{2}\right)^4 \\
&\quad \left. - A_A C_B^2 \sin(\Theta_{AB})^4 + C_B^2 \omega \sin(\Theta_{AB})^4 \right]. \quad (14)
\end{aligned}$$

$$\begin{aligned}
\langle S_A^{-n} S_A^{+n} \rangle &= u_A \Phi_A(T), \\
\langle S_B^{-n} S_B^{+n} \rangle &= u_B \Phi_B(T). \quad (15)
\end{aligned}$$

By varying $n=1, \dots, 2S_A$ and $n=1, \dots, 2S_B$, we obtain two independent sets of $2S_A$ and $2S_B$ equations, respectively. Following Tahir-Kheli and de ter Haar,⁸ we can write down $2S$ independent simultaneous linear equations in $\langle\langle S^z \rangle\rangle, \langle\langle S^{z2} \rangle\rangle, \langle\langle S^{z3} \rangle\rangle, \dots, \langle\langle S^{z2S} \rangle\rangle$. By putting n equal to $1, 2, \dots, 2S$, we show that

To determine $\langle S_i^{A-} S_j^{A+n} \rangle$, one defines $\Phi_{A(B)(T)}$ by

$$\begin{aligned}
\langle S_A^z \rangle &= \frac{[S_A - \Phi_A(T)][1 + \Phi_A(T)]^{(2S_A+1)} + [S_A + \Phi_A(T)][\Phi_A(T)]^{(2S_A+1)}}{[1 + \Phi_A(T)]^{(2S_A+1)} - [\Phi_A(T)]^{(2S_A+1)}}, \\
\langle S_B^z \rangle &= \frac{[S_B - \Phi_B(T)][1 + \Phi_B(T)]^{(2S_B+1)} + [S_B + \Phi_B(T)][\Phi_B(T)]^{(2S_B+1)}}{[1 + \Phi_B(T)]^{(2S_B+1)} - [\Phi_B(T)]^{(2S_B+1)}}. \quad (16)
\end{aligned}$$

The internal energy per atom is given by taking the average value of the Hamiltonian

$$\begin{aligned}
U &= \frac{1}{2} J_1 \sum_B \frac{1}{4} (\cos(\Theta_{AB}) - 1) (\langle S_A^+ S_B^+ + S_A^- S_B^- \rangle) + \frac{1}{4} (\cos(\Theta_{AB}) + 1) (\langle S_A^+ S_B^- + S_A^- S_B^+ \rangle) + \cos(\Theta_{AB}) \langle S_A^z \rangle \langle S_B^z \rangle \\
&\quad + \frac{1}{2} J_1 \sum_A \frac{1}{4} (\cos(\Theta_{AB}) - 1) (\langle S_B^+ S_A^+ + S_B^- S_A^- \rangle) + \frac{1}{4} (\cos(\Theta_{AB}) + 1) (\langle S_B^+ S_A^- + S_B^- S_A^+ \rangle) + \cos(\Theta_{AB}) \langle S_A^z \rangle \langle S_B^z \rangle \\
&\quad + \frac{1}{2} J_{2A} \sum_{\langle A \rangle_2} \frac{1}{4} 2 (\langle S_A^+ S_A^- + S_A^- S_A^+ \rangle) + \langle S_A^z \rangle^2 + \frac{1}{2} J_{2B} \sum_{\langle B \rangle_2} \frac{1}{4} [\cos(2\Theta_{AB}) - 1] (\langle S_B^+ S_B^- + S_B^- S_B^+ \rangle) + \frac{1}{4} [\cos(2\Theta_{AB}) + 1] \\
&\quad \times (\langle S_B^+ S_B^- + S_B^- S_B^+ \rangle) + \cos(2\Theta_{AB}) \langle S_B^z \rangle^2, \quad (17)
\end{aligned}$$

where the functions such as $\langle S_A^- S_A^+ \rangle$ are obtained by setting $n=1$ in Eq. (15).

Finally, the angle between each spin pair can be calculated in a self-consistent manner at any temperature within a first-order approximation. Strictly speaking, one has to minimize the free energy at each temperature to get the correct value of the angle. This is a formidable task. Instead, we limit ourselves in taking only the quantum fluctuations at $T=0$ into consideration and neglecting the thermal fluctuations. In doing so, the angle is obtained by minimizing U , instead of the free energy. This is in fact a mean-field-like approximation. We have then

$$\frac{\partial U}{\partial \Theta_{AB}} = 0. \quad (18)$$

In the zero-order approximation in $\langle S^\pm S^\pm \rangle$, one gets after some calculations for the noncollinear regime

$$\cos(\Theta_{AB}) = -\frac{2}{3} \frac{J_1 \langle S_A^z \rangle}{J_{2B} \langle S_B^z \rangle}. \quad (19)$$

For the collinear regime one has the solution $\Theta_{AB} = \pi$. In the first-order approximation in $\langle S^\pm S^\pm \rangle$, one has

$$\cos(\Theta_{AB}) = \frac{V_1}{V_2}, \quad (20)$$

where

$$\begin{aligned}
V_1 &= \sum_B \frac{J_1}{4} (\langle S_A^+ S_B^+ + S_A^- S_B^- \rangle) + \frac{J_1}{4} (\langle S_A^+ S_B^- + S_A^- S_B^+ \rangle) \\
&\quad + J_1 \langle S_A^z \rangle \langle S_B^z \rangle \sum_A \frac{J_1}{4} (\langle S_B^+ S_A^+ + S_B^- S_A^- \rangle) \\
&\quad + \frac{J_1}{4} (\langle S_B^+ S_A^- + S_B^- S_A^+ \rangle) + J_1 \langle S_A^z \rangle \langle S_B^z \rangle,
\end{aligned}$$

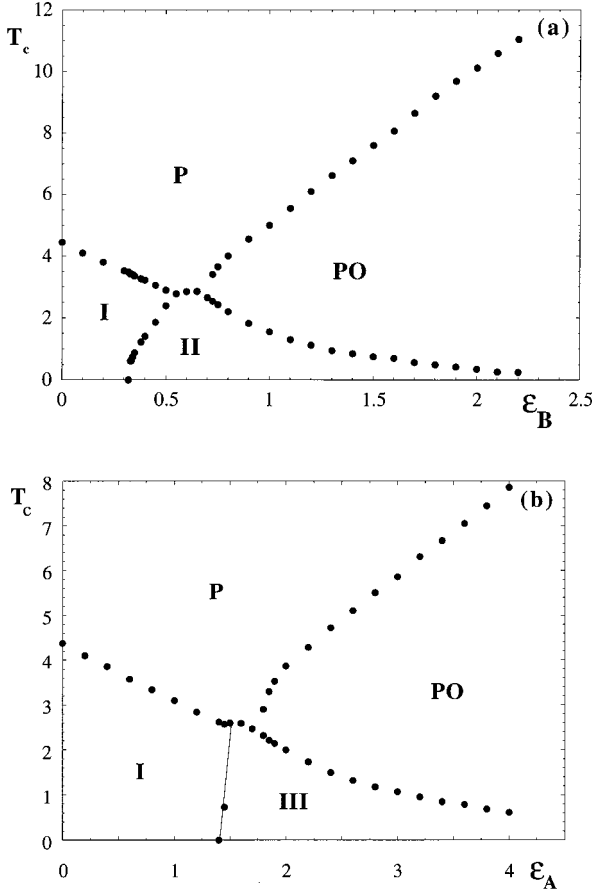


FIG. 3. (a) Phase diagram in the space (ϵ_B, T) for $S_A=1/2$, $S_B=1$, $\epsilon_A=0.2$, and $d/J_1=0.008$. (b) Phase diagram in the space (ϵ_A, T) for $S_A=1/2$, $S_B=1$, $\epsilon_B=0.1$ and $d/J_1=0.008$. Thin line separating phases I and III is a guide to the eye. P stands for paramagnetic phase, PO for partially ordered phase, I for collinear ‘‘ferrimagnetic’’ phase, and II and III for canted phases described by configurations II and III, respectively, of Fig. 2(b). See text for comments.

$$V_2 = - \sum_B J_{2B} (\langle S_B^+ S_B^+ + S_B^- S_B^- \rangle) + J_{2B} (\langle S_B^+ S_B^- + S_B^- S_B^+ \rangle) + 4J_{2B} \langle S_B^z \rangle^2. \quad (21)$$

The specific heat is obtained by taking numerical derivative of the internal energy with respect to T . The susceptibility is given by

$$\chi = \frac{\langle S^{z2} \rangle - \langle S^z \rangle^2}{T}, \quad (22)$$

where

$$\langle S^{z2} \rangle = S(S+1) - \langle S^z \rangle [1 + 2\Phi(T)], \quad (23)$$

with Φ being given by Eqs. (13) and (15).

III. RESULTS AND DISCUSSION

The above formalism can be applied to any set of parameters $(\epsilon_A, \epsilon_B, S_A, S_B, T)$. We show now two applications $S_A=1/2$, $S_B=1$, $\epsilon_A=0.2$, and $d/J_1=0.08$ with varying

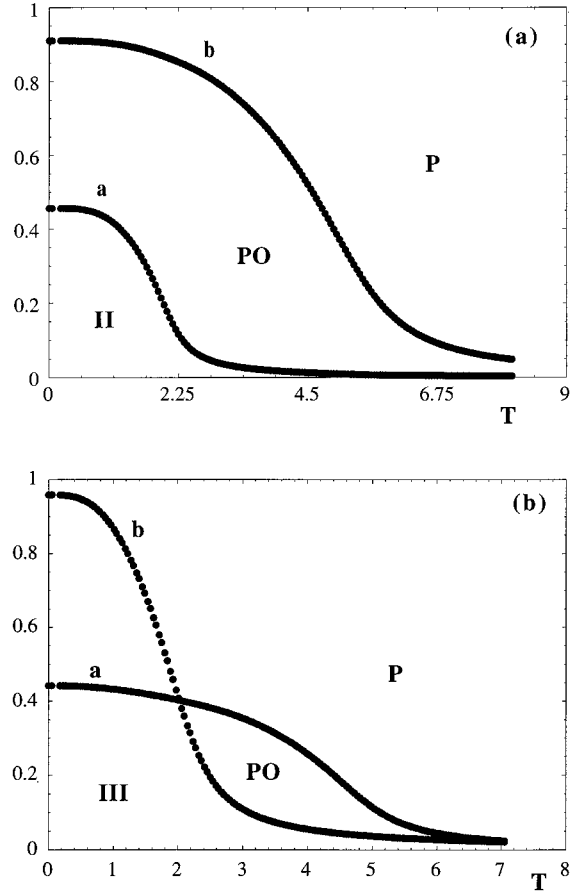


FIG. 4. (a) Local order parameters versus T for $\epsilon_A=0.2$ and $\epsilon_B=0.9$ (b) Local order parameters vs T for $\epsilon_B=0.1$ and $\epsilon_A=2.2$. The values of other parameters are the same as in Fig. 3. Curve a (b) is that of A (B) spins.

ϵ_B , for the first application, and $S_A=1/2$, $S_B=1$, $\epsilon_B=0.1$, and $d/J_1=0.008$ with varying ϵ_A , for the second application. The self-consistent numerical calculation is performed as follows: At $T=0$, we use $\langle S_A^z \rangle = 0.5$, $\langle S_B^z \rangle = 1$, and classical angle Θ as inputs to calculate the spin-wave spectrum which is then used to compute the Green functions. These functions are used next to calculate the outputs $\langle S_A^z \rangle$, $\langle S_B^z \rangle$, and Θ . One uses these outputs as inputs to repeat the calculations until one gets the self-consistent solution within a desired precision. Now we increase T and use the solution at $T=0$ as inputs and so on. Figures 3(a) and 3(b) display the general phase diagram in the space (ϵ_B, T) and (ϵ_A, T) , respectively. There are four phases in each application. Phase I corresponds to the collinear ‘‘ferrimagnetic’’ order (A spins and B spins are antiparallel). Phase II (III) is the canted ordering where A (B) spins are parallel and B (A) spins form an angle Θ_{AB} with A (B) spins and an angle $\Theta_{BB'}$ ($\Theta_{AA'}$) between two neighboring B (A) spins [see the description of zone II (III) in Fig. 2(a)]. Phase P is the paramagnetic phase. Phase PO (PO stands for partial ordering) is the most interesting phase discovered here for the first time: While the canted spins are still ordered, the parallel spins become disordered. This phenomenon has been seen until now in the *Ising* frustrated systems but never before in quantum spin systems (see Ref. 1). It is interesting at this stage to

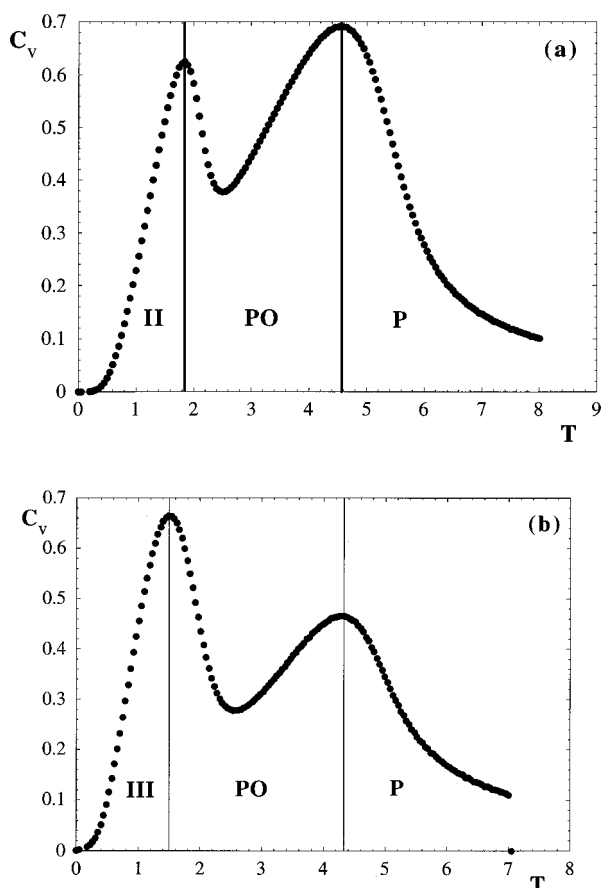


FIG. 5. (a) Specific heat per atom vs T for (a) $\epsilon_A=0.2$, $\epsilon_B=0.9$ and (b) $\epsilon_B=0.1$, $\epsilon_A=2.2$ (in unit of J_1/k_B). The values of other parameters are the same as in Fig. 3. The two peaks, at low and high T , correspond to the disordering of the parallel and canted spins, respectively. Zones II, III, P, and PO are defined in the caption of Fig. 3.

note that while the separation between phases I and II at $T=0$ is at $\epsilon_B=1/3$ [see Fig. 3(a)], the critical line issued

from this point is canted to the right at finite T : This means that the collinear configuration is favored at finite T in the range $\epsilon_B=1/3-0.6$ despite the fact that the spin configuration at low T is noncollinear in this range of ϵ_B . This may be due to the entropy effect which has been conjectured by Henley.¹⁰

Figure 4 shows an example of the local order parameters and the specific heat of the PO phase. In Fig. 4(a), the A -spin order parameter (curve a) becomes zero at some temperature well below the temperature where the B -spin order parameter (curve b) vanishes. However, in Fig. 4(b), it is the B -spin order parameter that vanishes at a lower temperature. Our conclusion is that in the two cases the order parameter of the “parallel” spins becomes zero at a temperature lower than that where the order parameter of noncollinear spins vanishes. In other words, only the sublattice with stronger interaction will remain ordered at high temperature.

In Fig. 5 we show the specific heat in the case when a partial disorder exists. The presence of two peaks in the specific heat in Fig. 5(a) [Fig. 5(b)] indicates the two transitions corresponding to the disordering of A spins (B spins) and B spins (A spins), respectively.

At this stage, we stress that while our formalism presented here allows us to calculate various physical properties of a frustrated mixed-spin system, the nature of the phase transition, i.e., the universality class, cannot be determined by our method. This is currently a controversial subject in the literature (see Ref. 1 for recent reviews). Finally, although we do not know at present if there are real systems which show partially disordered phases described by the model of this paper, we believe that our results can help experimentalists to understand their observations whenever they encounter such exotic phases. We note that some frustrated spin systems have been recently studied by many people.¹¹

ACKNOWLEDGMENT

The Groupe de Physique Statistique is an Equipe Postulante of CNRS (EP 127).

¹For recent reviews, see *Magnetic Systems with Competing Interactions (Frustrated Spin Systems)*, edited by H. T. Diep (World Scientific, Singapore, 1994).

²E. Callen, *Phys. Rev.* **150**, 367 (1966).

³H. T. Diep, I. Harada, and O. Nagai, *Phys. Lett.* **53A**, 157 (1975); H. T. Diep, *Phys. Status. Solidi B* **82**, 383 (1977).

⁴D. H. Lin and H. Zheng, *Phys. Rev. B* **37**, 5394 (1988).

⁵H. Zheng and D. H. Lin, *Phys. Rev. B* **37**, 9615 (1988).

⁶W.-Z. Shen and Z.-Y. Li, *Phys. Rev. B* **47**, 2636 (1993).

⁷P. Azaria, *J. Phys. C* **19**, 2773 (1985).

⁸R. A. Tahir-Kheli and D. ter Haar, *Phys. Rev.* **172**, 88 (1962).

⁹D. N. Zubarev, *Sov. Phys.* **3**, 320 (1960).

¹⁰C. Henley, *Phys. Rev. Lett.* **62**, 2056 (1989); *J. Appl. Phys.* **61**, 3962 (1987).

¹¹See review given by B. D. Gaulin in Ref. 1.